Supplementary Information

Feasible Strategy to Prepare Quantum Dot-Incorporated Carbon Nanofiber as Free-standing Platforms

Taeyoung Song,‡[a] Jun Young Cheong,‡[a] Ji Yong Choi,‡[b] Cheolmin Park,[c] Chulhee Lee,[a] Changsoo Lee,[a] Hyuck Mo Lee,[a] Sung-Yool Choi,[c] Hyunjoon Song,*[b] Il-Doo Kim*[a] and Duk Young Jeon*[a]

a. Department of Materials Science and Engineering, Korea Advanced Institute of Science and Technology, 291 Daehak-ro, Yuseong-gu, Daejeon 34141, Republic of Korea

b. Department of Chemistry, Korea Advanced Institute of Science and Technology, 291 Daehak-ro, Yuseong-gu, Daejeon 34141, Republic of Korea

c. School of Electrical Engineering, Center for Advanced Materials Discovery towards 3D Display, Graphene/2D Materials Research Center, Korea Advanced Institute of Science and Technology, 291 Daehak-ro, Yuseong-gu, Daejeon 34141, Korea.05-701, Republic of Korea.

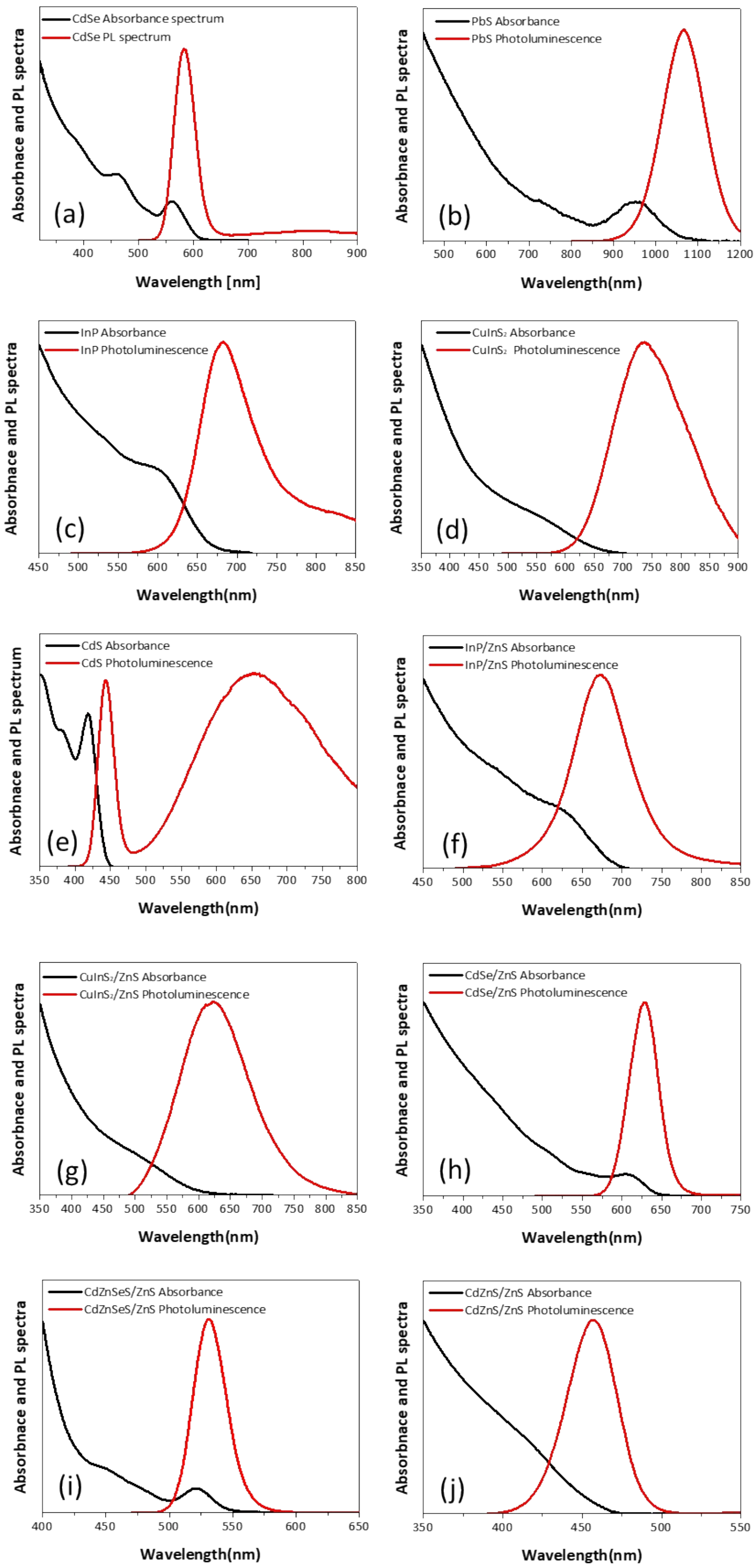

Fig. S1 Absorbance and PL spectra of various QDs: (a) CdSe, (b) PbS, (c) InP, (d) $CuInS_2$, (e) CdS, (f) InP/ZnS, (g) $CuInS_2$/ZnS, (h) CuSe/ZnS, (i) CdZnSeS/ZnS, and (j) CdZnS/ZnS.

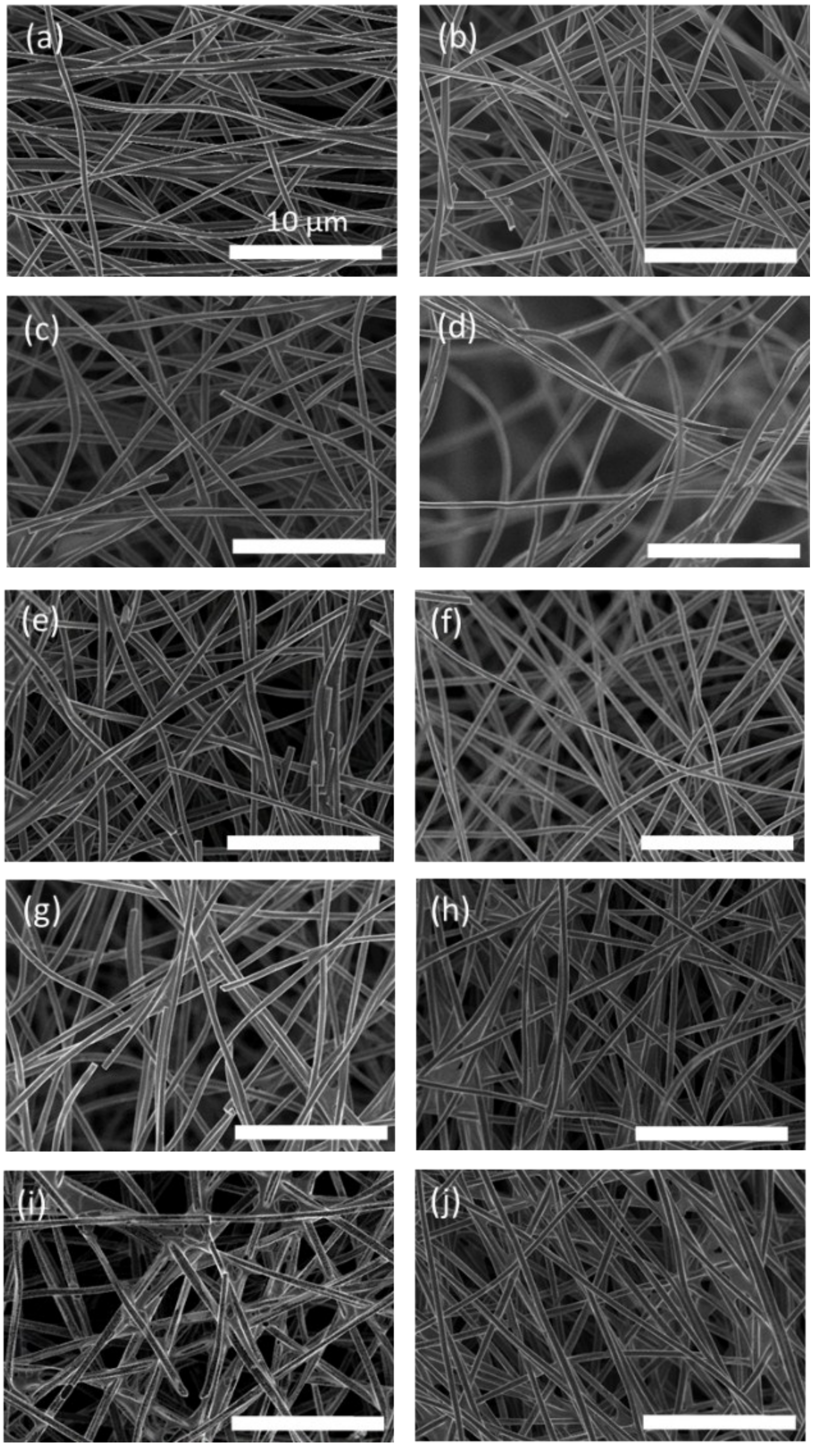

Fig. S2 Low magnification SEM images of QD-coated CNFs: (a) CdSe, (b) PbS, (c) InP, (d) $CuInS_2$, (e) CdS, (f) InP/ZnS, (g) $CuInS_2$/ZnS, (h) CdSe/ZnS, (i) CdZnSeS/ZnS, and (j) CdZnS/ZnS.

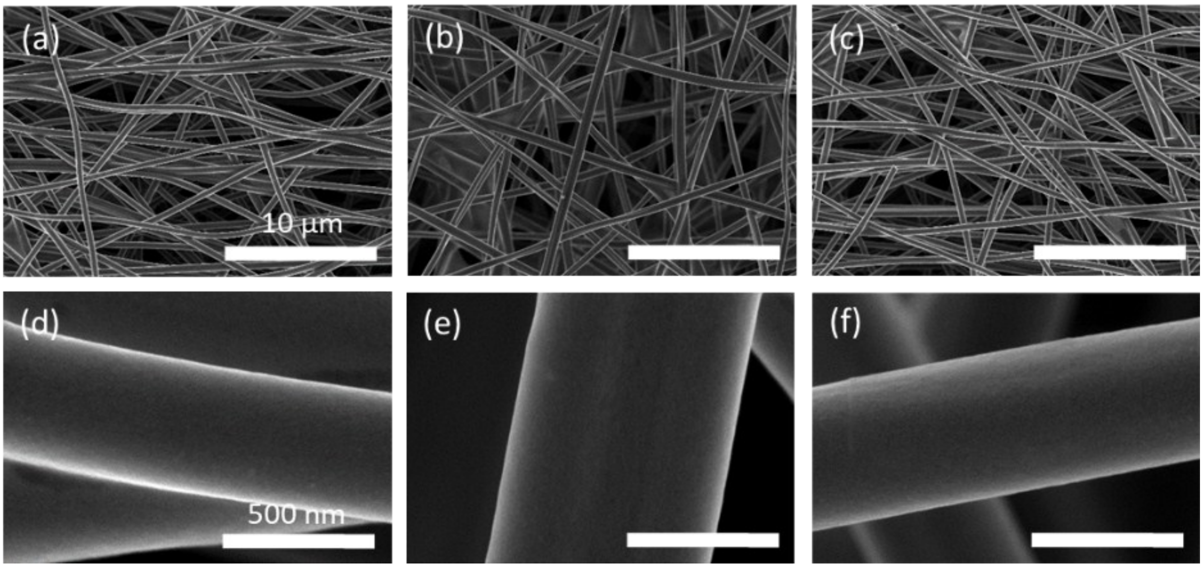

Fig. S3 Low magnification SEM images of CdSe-CNF with different concentrations of QD: (a) 20 mg ml^{-1}, (b) 50 mg ml^{-1}, and (c) 100 mg ml^{-1}. High magnification SEM images of CdSe-CNF with different concentrations of QDs: (d) 20 mg ml^{-1}, (e) 50 mg ml^{-1}, and (f) 100 mg ml^{-1}.

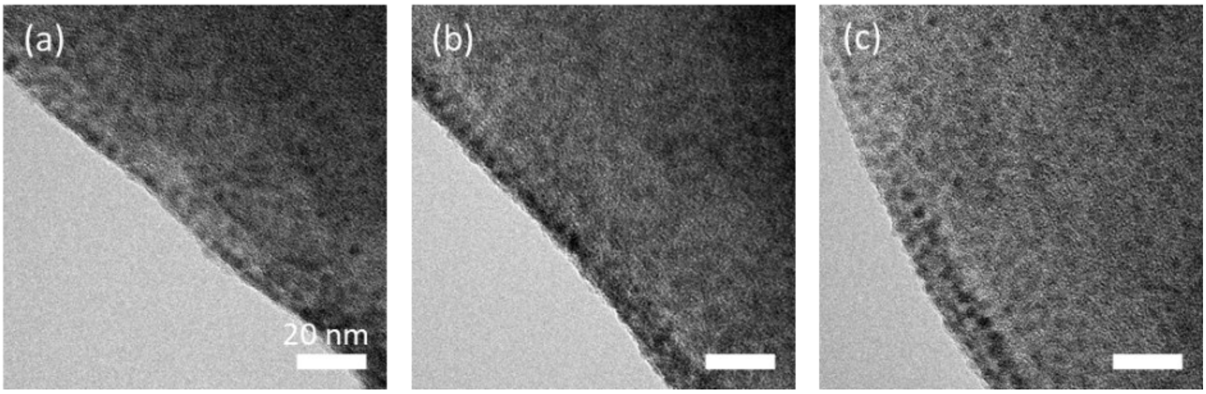

Fig. S5 TEM images of CdSe-CNF with different concentrations of QD: (a) 20 mg ml^{-1}, (b) 50 mg ml^{-1}, and (c) 100 mg ml^{-1}.

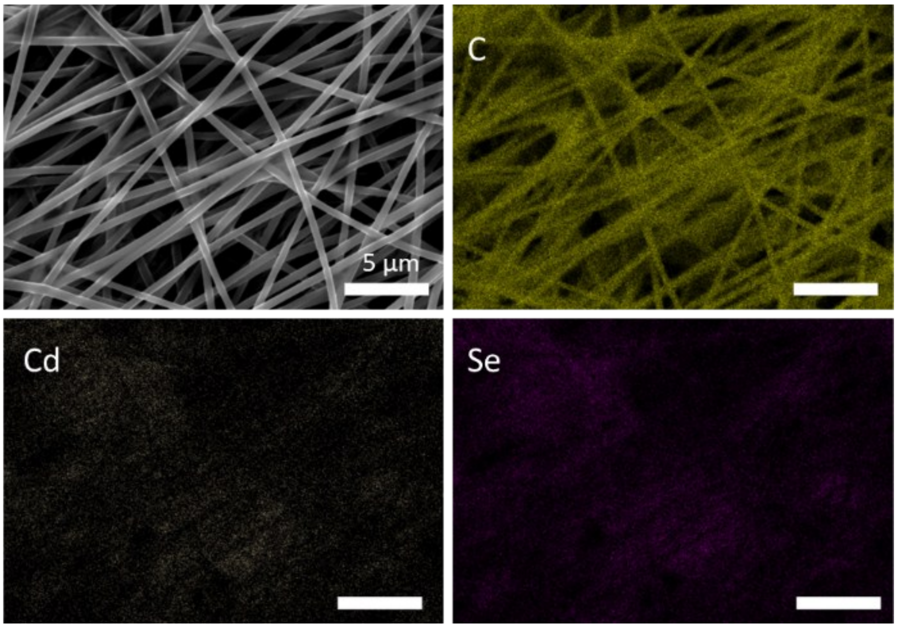

Fig. S4 SEM-EDS mapping of C, Cd, and Se for CdSe-CNF 20.

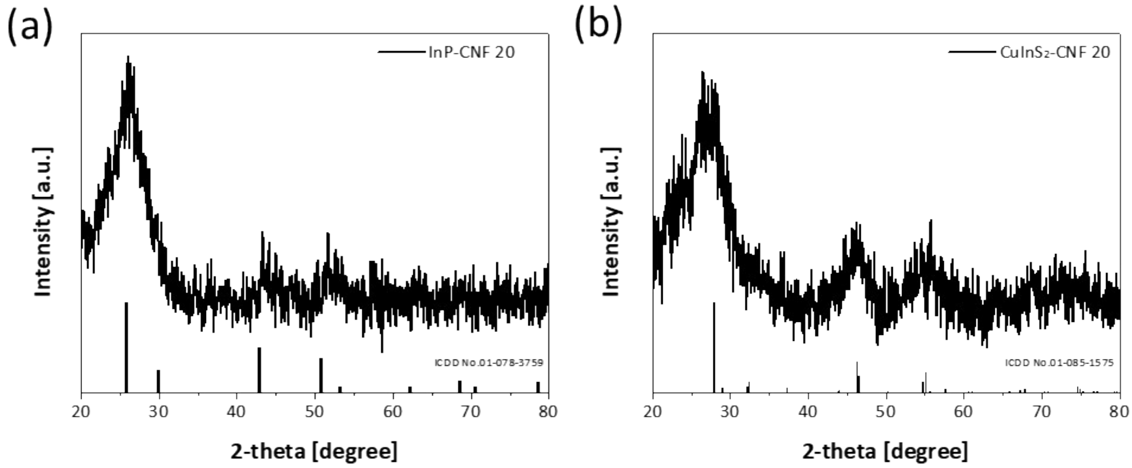

Fig. S7 XRD patterns of (a) InP-CNF, and (c) $CuInS_2$-CNF with the QD concentration of 20 mg ml^{-1}.

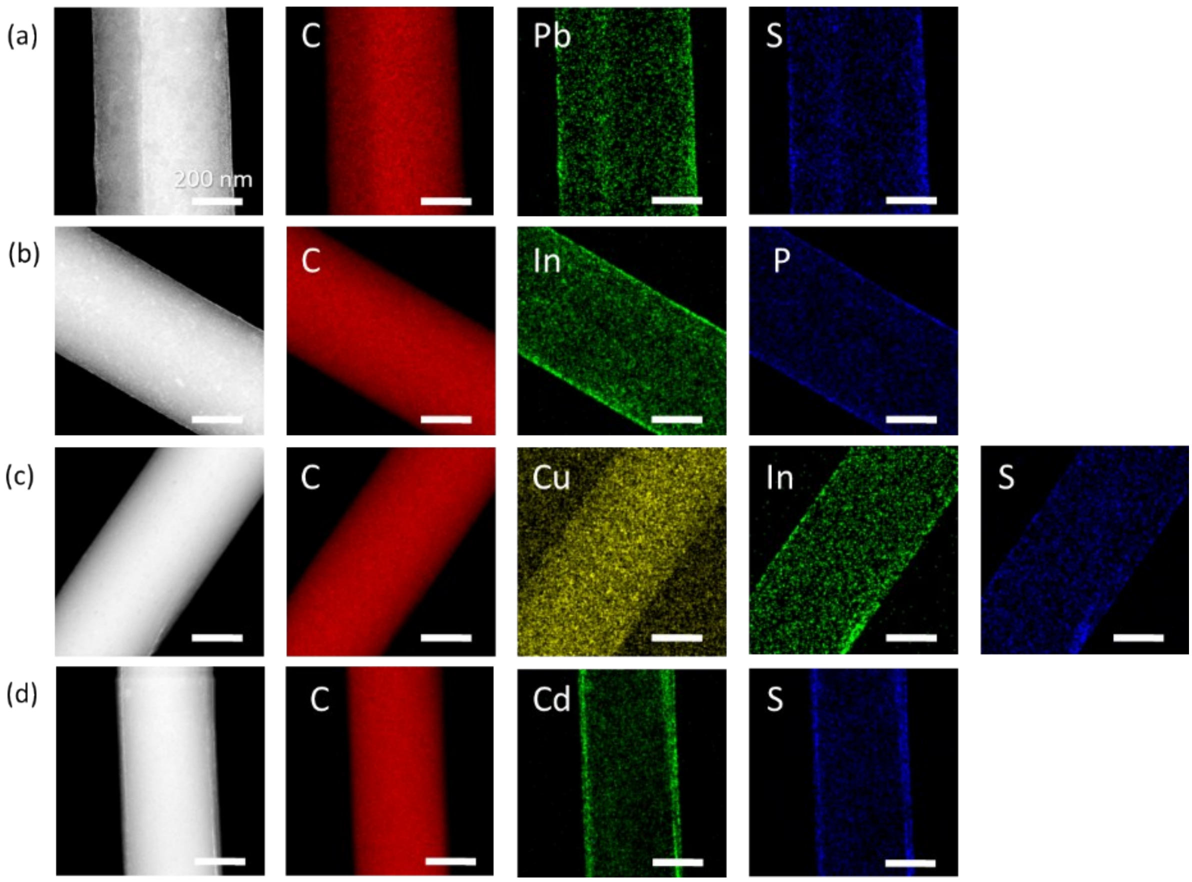

Fig. S6 TEM-EDS mapping of single component QD-coated CNFs: (a) PbS, (b) InP, (c) $CuInS_2$, and (d) CdS.

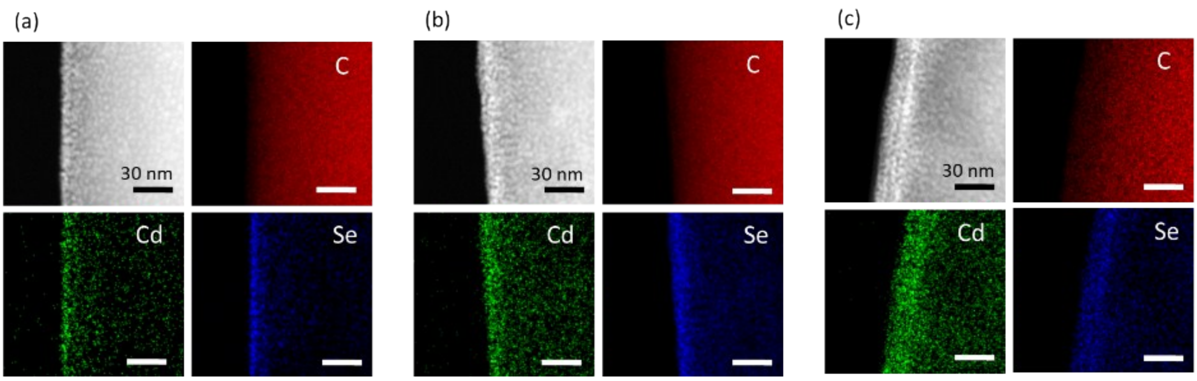

Fig. S8 TEM-EDS elemental mapping images of (a) CdSe-CNF 20, (b) CdSe-CNF 50, and (c) CdSe-CNF 100.

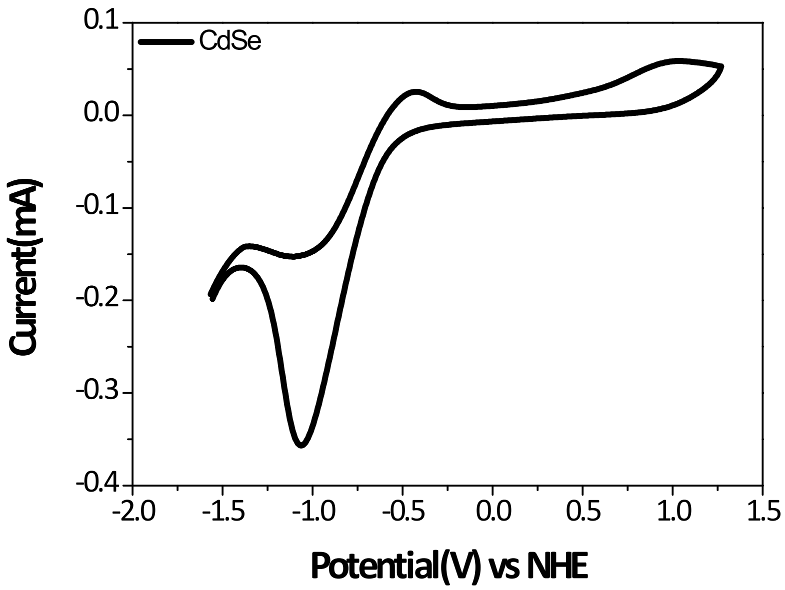

Fig. S9 CV curve of CdSe-CNF. The electrochemical measurement was analyzed using Metrohm Potentiostat/galvanostat (Interface 1000, Gamry). Pt disk electrode, Ag/AgCl and Pt-wire loop were used as working, quasi-reference, and counter electrodes, respectively. After fixing the electrodes to the cell, tetrabutylammonium perchlorate (171 mg) and CdSe QDs, dispersed in 5ml of dichloromethane (1mg ml^{-1}), were put in the cell. Then the potential with Ag/AgCl reference electrodes was calibrated with respect to the normal hydrogen electrode (NHE) with scan rate of 100 mV/s. The cathodic and anodic peaks at -1.06 V and 1.02 V were observed. Consequently, the HOMO level and LUMO level are -5.52 eV and -3.44 eV, respectively.

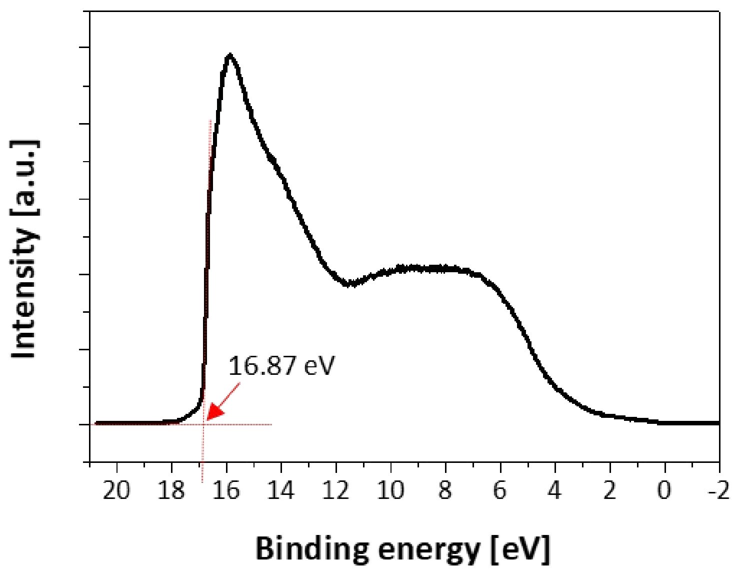

Fig. S10 UPS spectrum of the CNF using He I excitation.

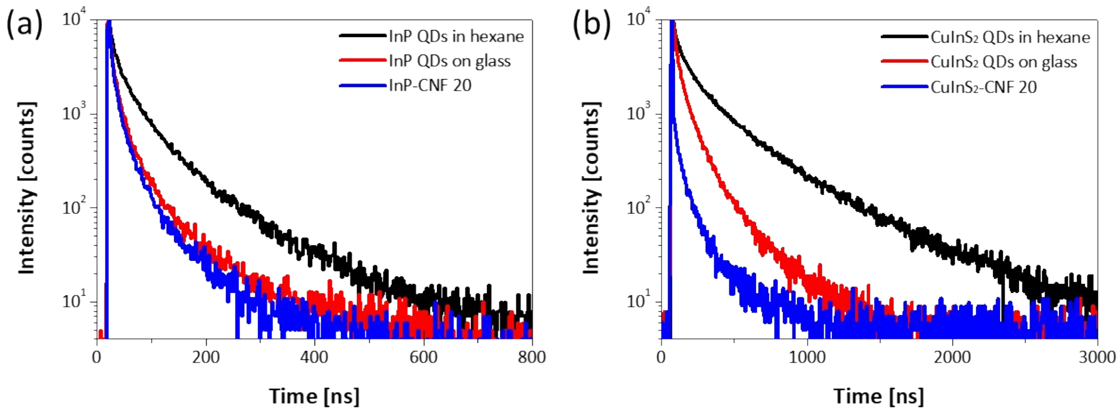

Fig. S11 Transient PL decay curves of (a) InP-CNF and (b) $CuInS_2$-CNF with the QDs concentration of 20 mg ml^{-1}.

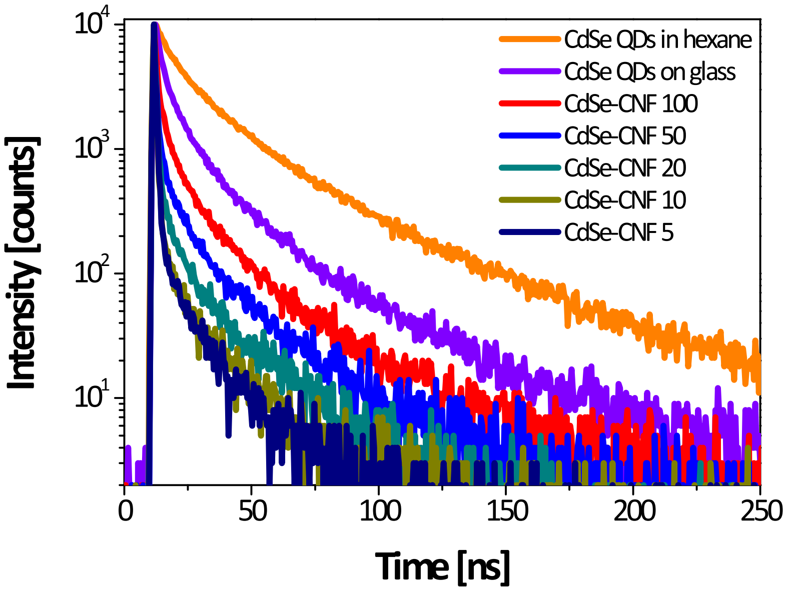

Fig. S12 Transient PL decay curves of CdSe-CNF with different QDs concentrations from 5 mg ml^{-1} to 100 mg ml^{-1}.

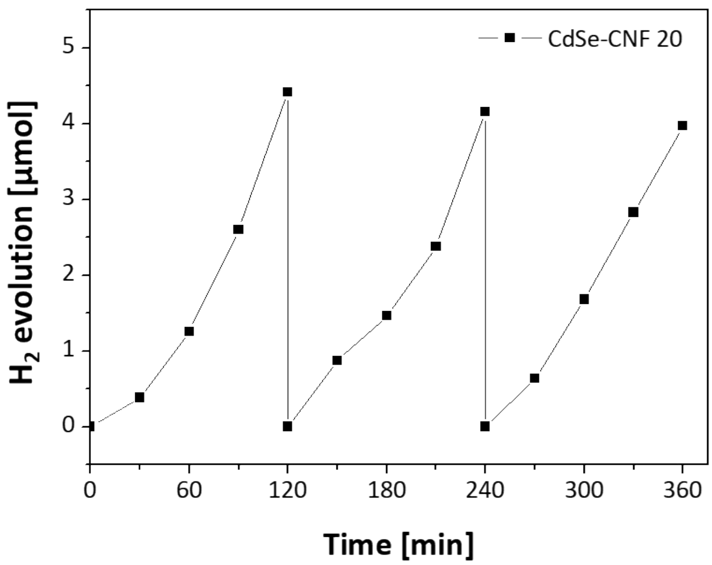

Fig. S13 Stability test of photocatalytic hydrogen evolution of the CdSe-CNF 20 in 0.25 M Na2S/0.35 M Na2SO3 aqueous solution under visible light (λ ≥ 420 nm)

Table S1 Average size of various QDs.

	Avg. size [nm]		Avg. size [nm]
CdSe	3.78	InP/ZnS	5.39
PbS	3.29	$CuInS_2$/ZnS	4.03
InP	2.76	CdSe/ZnS	5.63
$CuInS_2$	2.59	CdZnSeS/ZnS	11.74
CdS	2.93	CdZnS/ZnS	11.26

Fig. S14 (a) Schematic illustration on optoelectrical experiment. (b) Current-voltage (I-V) curve for CdSe-CNF 20 in dark and illumination. (c) The current ratios (I_{ph}/I_{dark}) of CdSe-CNF 20 depended on time under 5 Hz of laser on/off frequency at 1 V. The Optoelectrical data (I-V curve and response time measurement) were carried out according to following information. The QD-CNF samples were carefully contacted by two Au coated tip probes controlled by micro-positioners. The gap distance between the two tip probes was set to 80 µm. And 520 nm laser source (8.5 mW) was irradiated to the gap size (50 µm2) by defocusing 20 objective lens (NA 0.40). The on/off illumination for response time was chopped by an optical chopper system (300CD, Scitec Instruments). All of dark current, photocurrent and transient current were measured using a low-noise current preamplifier (SR570, Stanford Research Systems) at room temperature in the dark room.

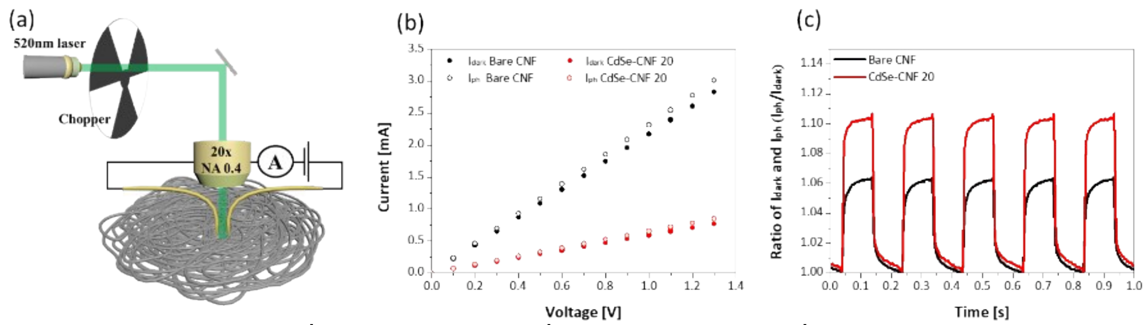

Table S2 The wt% of Cd, Se, and CdSe in different concentrations of CdSe-CNF.

	Cd [wt%]	Se [wt%]	CdSe [wt%]

20 mg ml^{-1}	4.56	1.25	5.81
50 mg ml^{-1}	7.72	2.12	9.84
100 mg ml^{-1}	10.95	2.97	13.92

Table S3 Fitting details on transient PL decay curves demonstrated in Figure S11.

InP	In hexane	On glass	InP-CNF 20
τ_1 [ns]	20.28	10.0	8.43
f_1 [%]	50.73	61.9	62.55
τ_2 [ns]	99.41	61.3	48.6
f_2 [%]	49.27	38.1	37.45
τ_{avg} [ns]	59.27	29.55	23.47

$CuInS_2$	In hexane	On glass	$CuInS_2$-CNF 20
τ_1 [ns]	86.51	38.33	9.14
f_1 [%]	37.38	53.09	45.86
τ_2 [ns]	440.77	171.24	105.18

f_2 [%]	62.62	46.91	54.14
τ_{avg} [ns]	308.35	100.68	61.14

Table S4 Fitting details on transient PL decay curves demonstrated in Figure 5b.

	CdSe-CNF 20	CdSe-CNF 10	CdSe-CNF 5
τ_1(ns)	0.97	0.76	0.84
f_1(%)	58.53	72.15	75.68
τ_2(ns)	16.32	15.25	13.77
f_2(%)	41.47	27.85	24.32
τ_{avg}(ns)[a]	7.34	4.80	3.98